VI International Conference on Computational Methods in Marine Engineering
MARINE 2015
F. Salvatore, R. Broglia and R. Muscari (Eds)

A REDUCED ORDER MODEL FOR THE SIMULATION OF MOORING CABLE DYNAMICS

Giovanni Stabile*†, Hermann G. Matthies† AND Claudio Borri*

*Dept. of Civil and Environmental Engineering
University of Florence
Via di Santa Marta 3, 50139 Florence, Italy
e-mail: giovanni.stabile@dicea.unifi.it, web page: http://www.dicea.unifi.it/

† Institute of Scientific Computing
Technische Universität Braunschweig
Hans-Sommer-Str. 65, 38106 Braunschweig, Germany
e-mail: wire@tu-bs.de - Web page: http://www.wire.tu-bs.de

Key words: Mooring Lines, Reduced Order Modelling, Fluid Structure Interaction, Vortex Induced Vibration

Abstract. In this paper the feasibility of a reduced order model (ROM) for the hydroelastic analysis of mooring lines is analysed. The local response of a piece of cable is studied through high fidelity fluid structure interaction (FSI) simulations. The high fidelity model is built by coupling a computational structural dynamics (CSD) solver with a computational fluid dynamics (CFD) solver using the approach of software components. The ROM is designed in such a way that it can be added to any beam element from a standard CSD solver. From the outside only the beam degrees of freedoms (DOFs) can be seen, the ROM DOFs are all internal.The local response of the cable is analysed and the feasibility of the ROM is discussed

1 INTRODUCTION

Long slender cylinders are found in many offshore applications and are the representative system for risers and mooring lines in deep water. The response of this kind of structure due to wave, current and tide loads may be complex, and phenomena such as vortex induced vibrations (VIV), unsteady lock-in, dual resonance, and travelling waves response may occur [1]. The methods used in the literature to solve the response analysis of long slender cylinders can be mainly divided into the following: experimental activities, semi empirical methods, and CFD methods. For more details one may refer to several review articles [2, 3, 4]. In this paper we will focus our attention on CFD methods, which

have demonstrated to be a promising way to capture the response of this kind of structure. They can be classified into two different classes:

- Full 3D simulations [5, 6], where the flow is discretized using three-dimensional elements. This approach has the advantage of capturing completely the three-dimensionality of the flow, but even with today's computational resources this is too demanding for the case of long cylinders and for flows with realistic values of the Reynold's number.

- Strip theories where the flow is modelled using bi-dimensional analysis at several different positions along the cable length. The flow at different planes is completely independent [7, 8, 9], and the three-dimensionality is only due to the structural model. This approach is computationally less demanding, and flow with realistic values of Reynold's number can be simulated. The disadvantage is that the three-dimensionality of the flow can not be captured, and forces at different planes have to be interpolated, and it is not easy to find a general way to perform such an interpolation.

In this paper the idea is to use the advantages of both methods. The response of the cable is studied only locally on a reduced domain size, which permits the use of a complete three-dimensional analysis with values of the Reynold's number suitable for practical applications. The logical process on which the ROM is based is summarized in Figure 1. A section of the cable, which is already three-dimensional, is subjected to an imposed motion with the same statistical characteristics as the response expected in full scale. The statistical characteristics of the motion in full scale could be carried out through full scale measurements (PHASE 3). In this paper, since full scale measurements were not available, the statistical properties of the imposed motion have been also obtained through high fidelity simulations on small scale size (PHASE 2). The cable has been retained at both ends with suitable springs which replace the remaining parts of the cable. The stiffness properties of the springs have been deduced from the FEM model in full scale (PHASE 1). It has been assumed that, in small scale, at the ends of the cable only transverse translations and bending rotations are relevant. This assumption does not limit in any way the motion of the cable in full scale which can move with all possible degrees of freedom. It is simply assumed that the fluid forces exerted on the cylinder due to the translation along its axis and due the rotation around its axis can be neglected. Once the statistical properties of the full scale motions are known one can create a random motion for each released degree of freedom. The so created random motions are imposed to the high fidelity small scale model, and the forces are measured (PHASE 3). The results of this analysis, varying the flow velocity and the flow inclination, may be used to feed a system identification technique that can be used to create a look-up table (PHASE 4). Such a look-up table once prepared could be added to any FEM solver. The additional DOFs are only internal and are identified trough a system identification technique. At

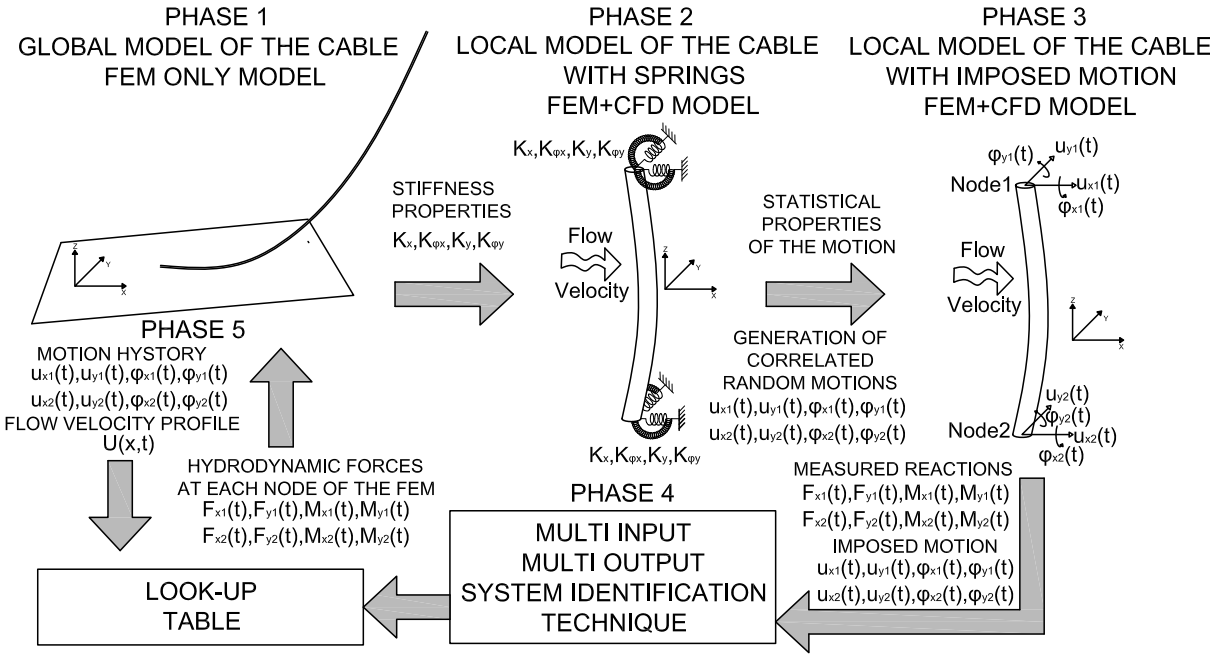

Figure 1: Flowchart of the discussed method

each time step, hydrodynamic forces, can be obtained simply calling the so developed finite element where only the instantaneous characteristics of motion are required. In this paper we focus our attention on phases 1 and 2 depicted in Figure 1.

2 THE COUPLED PROBLEM

The method described in the previous chapter is strongly based on the FSI small scale problem of phases 2 and 3. The coupled problem is here solved using a partitioned strategy with a direct force motion method (DFTM). In general a fluid structure interaction problem is formed by three different sub-problems: the fluid problem, the solid problem, and the mesh motion problem. The structural problem will be henceforth indicated with s while the fluid problem will be indicated with f. The solid problem is governed, in a spatial Lagrangian frame, by the momentum balance equation in terms of Cauchy stresses:

$$\boldsymbol{\nabla} \cdot \boldsymbol{\sigma} + \rho_s(\boldsymbol{b} - \ddot{\boldsymbol{u}}) = \boldsymbol{0} \text{ in } \Omega_s \times [0, T] \tag{1}$$

where $\boldsymbol{\sigma}$ is the Cauchy stress tensor, ρ_s is the solid density, $\boldsymbol{b}$ is the body force vector, $\ddot{\boldsymbol{u}}$ is the acceleration vector. Ω_s is the structural domain, and T is the length of the considered time window. A Newtonian, incompressible, viscous, isothermal and isotropic flow is considered. Since the fluid domain is not static but changing in time due to the deformation of the solid body we need to reformulate the Navier-Stokes equation for incompressible and viscous flows considering the motion of the FSI interface. This is done using an arbitrary-Lagrangian-Eulerian (ALE) [11] framework referenced to a frame

moving with a velocity $\boldsymbol{v_m}$. What we need to do is to replace inside the convective term the velocity $\boldsymbol{v}$ with the convective velocity $\boldsymbol{v_c} = \boldsymbol{v} - \boldsymbol{v_m}$, where $\boldsymbol{v_m}$ is the velocity of the moving part of the domain The momentum balance equation and the continuity equation, for the fluid domain, can be written in a spatial Eulerian frame as:

$$\begin{aligned} \frac{\partial \boldsymbol{v}}{\partial t} + (\boldsymbol{v_c} \cdot \boldsymbol{\nabla})\boldsymbol{v} - \nu \boldsymbol{\nabla}^2 \boldsymbol{v} = & \quad -\tfrac{1}{\rho_f}\boldsymbol{\nabla} p \quad \text{in } \Omega_f \times [0,T] \\ \boldsymbol{\nabla} \cdot \boldsymbol{v} = & \quad \mathbf{0} \qquad \text{in } \Omega_f \times [0,T] \end{aligned} \tag{2}$$

where $\boldsymbol{v}$ is the flow velocity vector, t is the time, ν is the flow viscosity, and p is the pressure. Ω_f is the fluid domain, and T is the length of the considered time window. In the present work the solid and the fluid problem are solved using different space discretization techniques. The solid problem is solved using finite elements, while the fluid problem is solved using finite volumes. The mesh motion problem is solved imposing the matching of velocities and stresses at the FSI interface:

$$\begin{aligned} \boldsymbol{v_s} = \boldsymbol{v_f} \text{ on } \partial\Omega_{FSI} \times [0,T] \\ \boldsymbol{n} \cdot \boldsymbol{\sigma} = -p\boldsymbol{n} + 2\nu(\boldsymbol{n} \cdot \boldsymbol{\nabla^S})\boldsymbol{v_f} \text{ on } \partial\Omega_{FSI} \times [0,T] \end{aligned} \tag{3}$$

where $\boldsymbol{n}$ is the FSI-interface normal vector, $\boldsymbol{\nabla^S}$ is the symmetric part of the gradient operator. The matching of variables at the interface is enforced with an implicit scheme which conserves the energy at the interface. For each time step of the coupled simulation $t_{c,i}$ an iterative cycle on the velocity residual is performed until the achievement of a desired tolerance:

$$\boldsymbol{res} = \boldsymbol{v_{s,i}} - \boldsymbol{v_{f,N}} \leq TOL \tag{4}$$

The iterative scheme is realized using a block Gauss-Seidel procedure reported in Algorithm 1 [15]. The time step size of the fluid sub-problem may be different to the time step size of the solid sub-problem. The only requirement is that each sub-problem has to be performed the sufficient number of times necessary to reach the time step size of the coupled simulation. Inside the algorithm the term ω is a scalar value obtained by Aitken's relaxation [12]. The procedure will work with any CFD solver and any CSD solver which can be coupled properly, here the solid sub-problem is solved using the FEM solver FEAP [13], while the fluid sub-problem is solved using the FVM solver OpenFOAM [14]. The coupling is realized using the approach of software components and the component template library (CTL) [15] is used as common middleware. Here the features of the FSI solver are reported only briefly, for additional details please refer to [16].

Algorithm 1 Coupling algorithm

Given: initial time T_0, length of the simulation T, time step size of the fluid simulation Δt_f, time step size of the solid simulation Δt_s, time step size of the the coupled simulation Δt_c, the tolerance TOL

while $t < T$ **do**
  $k = 0, \omega^{(0)} = \omega_0$
  while $\boldsymbol{res}_{\boldsymbol{N+1}}^{\boldsymbol{(k)}} < TOL$ **do**
    if $k > 0$ **then**
      $\omega^{(k)} = -\omega^{(k-1)} \frac{\boldsymbol{res}_{N+1}^{(k-1)} \cdot (\boldsymbol{res}_{N+1}^{(k)} - \boldsymbol{res}_{N+1}^{(k-1)})}{\left\| \boldsymbol{res}_{N+1}^{(k)} - \boldsymbol{res}_{N+1}^{(k-1)} \right\|^2}$
    end if
    Predict fluid velocities at the interface: $\boldsymbol{V}_{\boldsymbol{f},\boldsymbol{N+1}}^{\boldsymbol{(k)}} = P(\boldsymbol{V}_{\boldsymbol{N}}^{(\boldsymbol{k_{max}})}, \boldsymbol{V}_{\boldsymbol{N-1}}^{(\boldsymbol{k_{max}})}, \dots)$
    Given $\boldsymbol{V}_{\boldsymbol{f},\boldsymbol{N+1}}^{\boldsymbol{(k)}}$ solve the fluid problem in ALE formulation $\rightarrow \boldsymbol{F}_{\boldsymbol{f},\boldsymbol{N+1}}^{\boldsymbol{(k)}}$
    Given $\boldsymbol{F}_{\boldsymbol{f},\boldsymbol{N+1}}^{\boldsymbol{(k)}}$ solve the solid problem $\rightarrow \boldsymbol{V}_{\boldsymbol{S},\boldsymbol{N+1}}^{\boldsymbol{(k)}}$
    Evaluate residual $\boldsymbol{res}_{\boldsymbol{N+1}}^{\boldsymbol{(k)}} = \boldsymbol{V}_{\boldsymbol{S},\boldsymbol{N+1}}^{\boldsymbol{(k)}} - \boldsymbol{V}_{\boldsymbol{f},\boldsymbol{N+1}}^{\boldsymbol{(k)}}$
    Update fluid velocity at the interface $\boldsymbol{V}_{\boldsymbol{f},\boldsymbol{N+1}}^{\boldsymbol{(k+1)}} = \boldsymbol{V}_{\boldsymbol{S},\boldsymbol{N+1}}^{\boldsymbol{(k)}} + \omega^{(k)} \boldsymbol{res}_{\boldsymbol{N+1}}^{\boldsymbol{(k)}}$
    $k = k + 1$;
  end while
  $N = N + 1, t = t + \Delta t_c$
end while

2.1 The Fluid Sub-Problem

The fluid computation has been carried out using a large eddy simulation (LES) turbulence model [17]. This approach has demonstrated to be particularly suitable to analyse the flow around a circular cylinder especially in the range of Reynold's numbers interesting for practical applications [18]. The sub grid scale model is a $k-$equation eddy viscosity model. The mesh is represented in Figure 2 and is structured using a polar distributed grid in the proximity of the cylinder and a Cartesian distributed grid in the other regions. The region near to the wall has been refined, and along the vertical direction an equally spaced mesh has been used ($\Delta z \approx \mathrm{D}/2$).

The distance of the cylinder from the inlet is equal to $8D$, the distance from the outlet is equal to $15D$, and the domain width is equal to $20D$. The diameter of the cylinder is equal to $D = 0.102$m, which is a common diameter for mooring line cables available on the market. The domain height is equal to $40D$. The height of the domain has been chosen in order to make the structure slender enough to be modelled using a beam theory. The flow has a constant uniform velocity at the inlet and constant zero pressure value at the outlet. Sides are modelled with slip conditions, and the lower and upper part are modelled as symmetry planes. The PIMPLE algorithm [14] and an Euler implicit scheme with a time step $\Delta t_f = 0.001$s are used. The fluid is water with a density of $\rho_f = 10^3 \mathrm{kg/m^3}$ and kinematic viscosity of $\nu_f = 1 \times 10^{-6} \mathrm{m^2/s}$.

The reliability of the present method is strongly correlated to the reliability of the fluid computation. For this reason, in order to validate the whole model, the first step is to validate the small scale model and the CFD solver. Results have been compared to numerical and experimental data in terms of lift, drag, and Strouhal number.

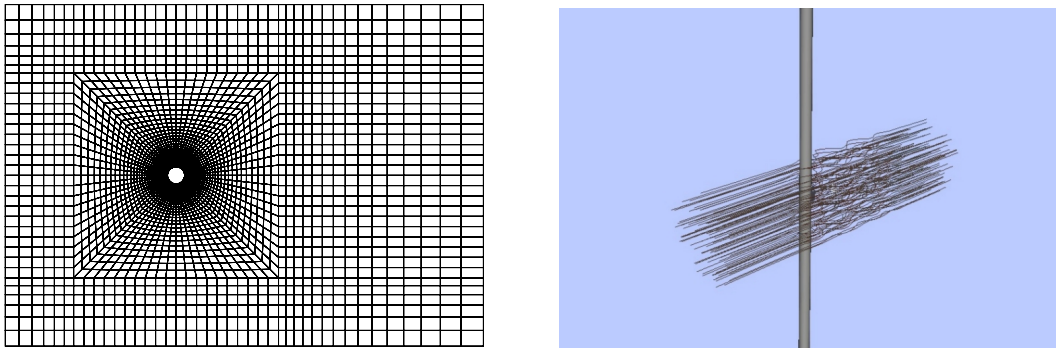

(a) top view of the mesh (b) View of the cylinder with stream-lines

Figure 2: Domain of the simulation

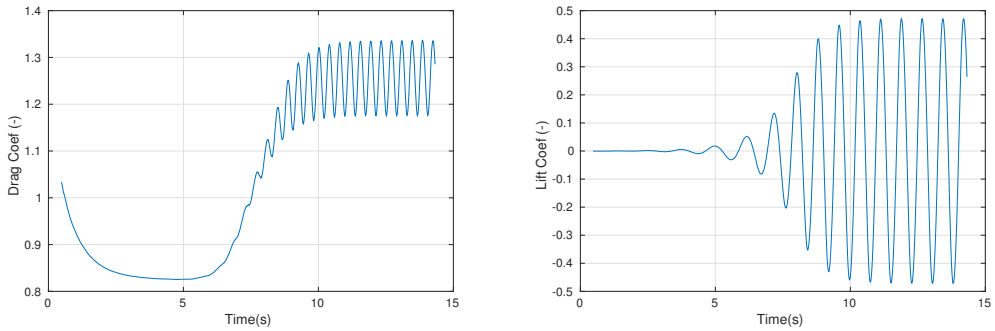

Figure 3: Time evolution of drag and lift coefficients

Lift and drag forces are described in terms of the drag coefficient and lift coefficient:

$$C_D = \frac{F_D}{0.5\rho U^2 D} \qquad (5)$$
$$C_L = \frac{F_L}{0.5\rho U^2 D}$$

where F_D and F_L are the drag and lift force per unit of length respectively, U is the free stream velocity of the flow. In Figure 3 the time evolution of the lift and drag coefficient is reported. All the results are carried out using a Reynold's number $Re = 6.31 \times 10^4$ which matches the result of the benchmark from [18]. The results are compared to the same benchmark case in terms of root mean square (RMS) of the lift coefficient, mean drag coefficient, and Strouhal number. As we can see from Table 1, results match well with experimental and previous numerical results.

2.2 The Solid Sub-Problem

Since we are not interested in the accurate modelling of the stresses inside the cylinder but rather on the global response of the cable, the structure has been modelled using a

Table 1: Comparison with literature- and experimental values from [18]

	RMS LC	MEAN DC	ST
Exp. Value	0.24	1.16	0.19
Present	0.33	1.25	0.20
A	0.53	0.70	0.28
B	0.47	0.87	0.25
C	0.83	1.05	0.25
D	0.60	1.37	0.18
E	0.18	1.10	0.28
F	0.51	1.49	0.20
G	0.86	1.14	0.24
H1	1.08	1.28	0.29
H2	0.10	0.54	0.35
H3	0.58	1.38	0.22
H4	0.99	1.70	0.21

geometrically exact beam element based on [19]. The time integration has been performed using a generalized HHT-α integration scheme [20] which has been demonstrated to be enough accurate for the specific case. The structure has been discretized with 40 equally spaced finite elements with the same spacing used for the fluid sub-problem. The same time step size of the fluid sub-problem $\Delta t_s = 0.001$s has been used. The structure has a cylindrical cross section with diameter $D = 0.102$m, density $\rho_s = 5.582 \times 10^3 \text{kg/m}^3$, Young's modulus $E_s = 5.88 \times 10^8 \text{N/m}^2$, and Poisson's ratio $\nu_s = 0.3$.

2.3 The Mesh Motion Problem

The coupling of the fluid and the solid problems has been realized in a strong way using a Block Gauss-Seidel coupling algorithm. The time step of the fluid problem has been imposed to be equal to the time step of the solid problem. At each time step we need to update the mesh of the fluid problem using the displacement coming from the solid computation, and on the other hand we need to transfer forces deriving from the fluid computation to the structure. This procedure is not always simple, because most of the time we have to deal with not-matching meshes, and in our case we even have different spatial dimensions for the models. The beam is in fact a mono-dimensional object, while the fluid forces are evaluated on the FSI interface, which is a 2-D surface in three-dimensional space. So the forces coming from the fluid mesh have to be properly converted into line forces. The problem is solved making the hypotheses of a non-deformable cross sections and fluid forces are obtained by circumferential integration and are transferred to the beam nodes through the shape functions of the beam. The adjoint procedure has been used to move the points of the FSI interface starting from the nodal displacement of the beam. Points of the fluid mesh which do not belong to the FSI interface are moved according to a Laplacian smoothing algorithm [14]: the equation of cell motion is solved based on the Laplacian of the diffusivity and the cell displacements. The diffusivity field

is based quadratically on the inverse of the cell center distance to the FSI interface.

3 DISCUSSION

In this section some preliminary results of the small scale model and the discussion about the important aspects we should keep in mind in the development of the ROM are presented.

3.1 Hysteretic Effects

One important feature regarding the force exerted by the fluid on a section of the cable is the hysteresis of the system. What is happening at a certain time step depends in fact not only on the instantaneous characteristic of the relative motion between the flow and the cable, but also on what happened at previous time steps. In the development of a ROM it is important to consider also this effect.

Two identical simulations with different initial conditions have been performed, in order to understand the size of the time window we have to consider for the ROM. The two simulations both consider a rigid circular cylinder perpendicular to a flow with a uniform constant velocity equal to 0.5m/s. The other parameters of the simulation are identical to the ones used in Section 2. Both cylinders are subjected to a random imposed motion in cross-flow and in-line direction. The random motion has been created using a narrow band spectrum with a main frequency equal to the Strouhal frequency for the cross-flow direction, and twice the Strouhal frequency for the in-line direction. The imposed motion is started after 5s of simulation. In the first case the cylinder is at rest until the beginning of the random imposed motion, while in the second case an initial disturbance is introduced. Forces in in-line and cross-flow direction are evaluated and the results are plotted in Figure 4. The blue line represents the cylinder with an initial disturbance, and the red line represents the cylinder without disturbance. In the lower part of the graph the imposed motion for both cylinders is represented. Results are presented for both the in-line and the cross-flow directions. For the first five seconds after the beginning of the imposed motion the measured forces are quite different, but after the first five seconds the forces are almost identical.

3.2 Spring Supported Model

As reported in Section 1 a possible way to find a suitable imposed motion for the small scale problem can be to run an FSI simulation of the model supported by springs which simulate the full scale behaviour of the cable. The stiffness properties have been deduced from the FEM full scale model. The FEM full scale model is built using the same structural properties of the FSI model. The cable is hinged at both ends and the contact with the ground has been modelled using a penalty method approach. Firstly the catenary shape of the cable is found performing an analysis with gravity loads only, then a load F for each released degree of freedom is applied and the displacement S is

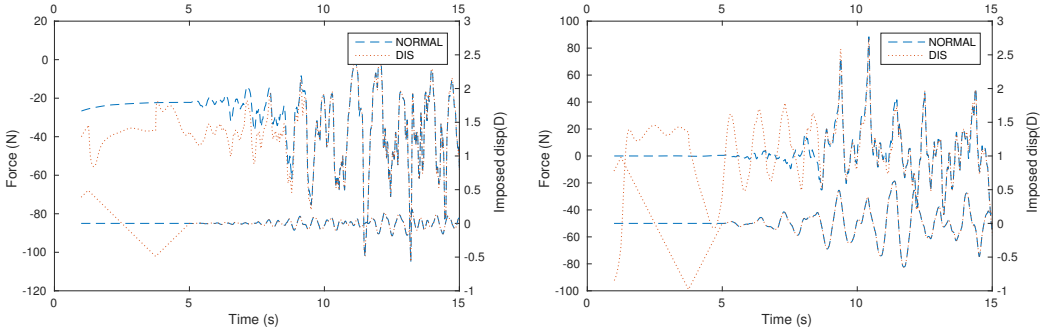

Figure 4: Memory effect in in-line and cross-flow direction

measured. By operating in such a manner it is possible to deduce an equivalent linear stiffness for each released degree of freedom simply by dividing the applied load by the relative displacement $K_i = F_i/S_i$. The so obtained stiffness are equal to:

$$\begin{aligned} K_x &= 576\text{N/m} \; K_{\varphi x} = 803\text{Nm/rad} \\ K_y &= 409\text{N/m} \; K_{\varphi y} = 10417\text{Nm/rad} \end{aligned} \tag{6}$$

An FSI simulation with the same parameters as discussed in Section 2 is performed, and the displacements at both ends of the cable are measured. The flow velocity at the inlet is equal to $V = 0.5$m/s. This phase is important to understand the statistical properties that an imposed motion at both ends should have and to verify the ability of the present small scale model to reproduce the full scale behaviour. Results are reported in time and frequency domain in Figures 5 and 6. The DC component has been subtracted from the results. It is interesting to notice that the in-line displacements at the ends are in-phase at both ends while the cross-flow displacement is π rad out of phase. It means that the cable is vibrating in a way that in full scale it would be represented by a travelling wave. In Figure 6 the one-sided power spectral density (PSD) of the measured displacements and rotations are plotted. The spectra resemble quite well the behaviour which is normally observed in real full scale measurements. In the in-line displacements spectrum we can observe two peaks, the first peak is close to the natural frequency of the system $f_{N_{IL}} = 0.4$Hz while the second peak is close to twice the Strouhal frequency $f_{St} = St \cdot D/U = 1$Hz. For the cross-flow displacement we observe a similar behaviour but with a smaller first peak. As expected the second peak has a frequency close to the Strouhal frequency. In the time domain plot we can observe that rotations have a relatively small value.

4 CONCLUSIONS AND NEXT STEPS

Results of FSI simulations of a piece of cable inside a uniform current are presented. The present model can be used in future works to develope a ROM that could dramatically

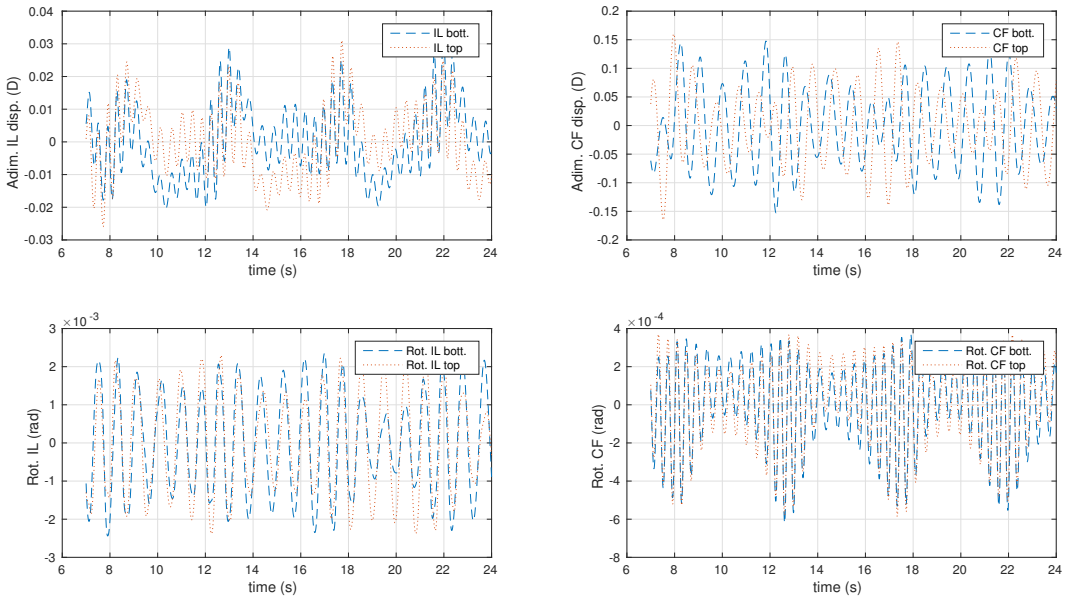

Figure 5: Results of the spring supported model in the time domain

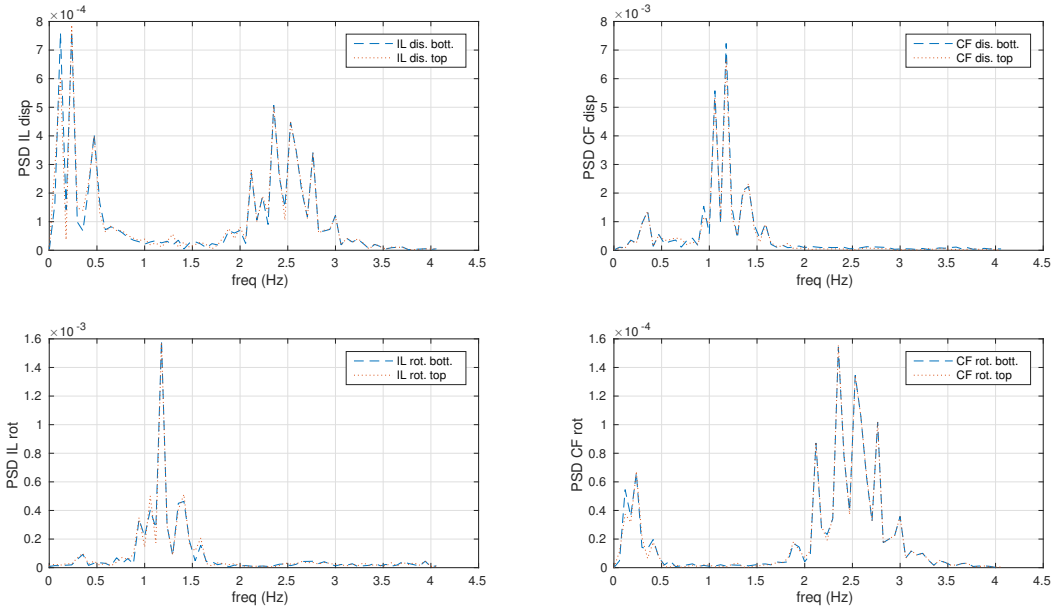

Figure 6: Results of the spring supported model in the frequency domain

reduce the computational cost of the simulation. The CFD code used in the FSI model has been validated with experimental and numerical results showing a good accordance. The hysteretic effects of the VIV phenomena has been analyzed, and for the particular case it shows a memory of approximately 5s. A spring supported model has been analysed in order to understand the statistical properties that an imposed motion at the ends of the small scale model should have. The response spectrum of the spring supported model confirms what is normally observed in full scale real problems. The next steps are the creation of a new FSI model with an imposed motion with the same statistical properties of the spring supported model results and the measurements of the relative forces at both ends. The results of this analysis will be used to feed a system identification technique in order to get the dynamical properties of the ROM.

REFERENCES

[1] X. Wu, F. Ge, and Y. Hong, "A review of recent studies on vortex-induced vibrations of long slender cylinders," *Journal of Fluids and Structures*, vol. 28, pp. 292–308, 2012.

[2] P. Bearman, "Circular cylinder wakes and vortex-induced vibrations," *Journal of Fluids and Structures*, vol. 27, no. 5, pp. 648–658, 2011.

[3] R. Gabbai and H. Benaroya, "An overview of modeling and experiments of vortex-induced vibration of circular cylinders," *Journal of Sound and Vibration*, vol. 282, no. 3, pp. 575–616, 2005.

[4] C. Williamson and R. Govardhan, "A brief review of recent results in vortex-induced vibrations," *Journal of Wind Engineering and Industrial Aerodynamics*, vol. 96, no. 6, pp. 713–735, 2008.

[5] D. J. Newman and G. E. Karniadakis, "A direct numerical simulation study of flow past a freely vibrating cable," *Journal of Fluid Mechanics*, vol. 344, pp. 95–136, 1997.

[6] R. Bourguet, G. E. Karniadakis, and M. S. Triantafyllou, "Lock-in of the vortex-induced vibrations of a long tensioned beam in shear flow," *Journal of Fluids and Structures*, vol. 27, no. 5, pp. 838–847, 2011.

[7] T. Kvamsdal, J. Amundsen, and K. Okstad, "Numerical methods for fluid–structure interactions of slender structures," in *Proceedings of ECCM*, vol. 99, Citeseer, 1999.

[8] K. Huang, H.-C. Chen, C.-R. Chen, *et al.*, "Riser VIV analysis by a CFD approach," in *Proceedings of the 17th International Offshore and Polar Engineering (ISOPE) Conference, Lisbon, Portugal*, 2007.

[9] C. Yamamoto, J. Meneghini, F. Saltara, R. Fregonesi, and J. Ferrari, "Numerical simulations of vortex-induced vibration on flexible cylinders," *Journal of fluids and structures*, vol. 19, no. 4, pp. 467–489, 2004.

[10] P. Mainçon, "A Wiener-Laguerre model of VIV forces given recent cylinder velocities," *Mathematical Problems in Engineering*, vol. 2011, 2011.

[11] J. Donea, S. Giuliani, and J. Halleux, "An arbitrary lagrangian-eulerian finite element method for transient dynamic fluid-structure interactions," *Computer methods in applied mechanics and engineering*, vol. 33, no. 1, pp. 689–723, 1982.

[12] U. Küttler and W. A. Wall, "Fixed-point fluid–structure interaction solvers with dynamic relaxation," *Computational Mechanics*, vol. 43, no. 1, pp. 61–72, 2008.

[13] R. Taylor, "Feap. a finite element analysis program. user manual, version 8.2," *University of California at Berkeley*, 2008.

[14] H. Jasak, A. Jemcov, and Z. Tukovic, "Openfoam: A c++ library for complex physics simulations," 2013.

[15] H. G. Matthies, R. Niekamp, and J. Steindorf, "Algorithms for strong coupling procedures," *Computer methods in applied mechanics and engineering*, vol. 195, no. 17, pp. 2028–2049, 2006.

[16] A. Ibrahimbegovic, R. Niekamp, C. Kassiotis, D. Markovic, and H. G. Matthies, "Code-coupling strategy for efficient development of computer software in multiscale and multiphysics nonlinear evolution problems in computational mechanics," *Advances in Engineering Software*, vol. 72, pp. 8–17, 2014.

[17] P. Sagaut, *Large Eddy Simulations for Incompressible Flows*, vol. 3. Springer Berlin, 2000.

[18] W. Qiu, H. Lie, J. Rousset, S. Sphaier, L. Tao, X. Wang, T. Mikami, and V. Magarovskii, "Report of the Ocean Engineering Committee," in *27th International Towing Tank Conference*, pp. 1–74, 2014.

[19] J. C. Simo and L. Vu-Quoc, "On the dynamics in space of rods undergoing large motions: a geometrically exact approach," *Computer methods in applied mechanics and engineering*, vol. 66, no. 2, pp. 125–161, 1988.

[20] H. M. Hilber, T. J. Hughes, and R. L. Taylor, "Improved numerical dissipation for time integration algorithms in structural dynamics," *Earthquake Engineering & Structural Dynamics*, vol. 5, no. 3, pp. 283–292, 1977.